2D characterization of type-II Edge Localized Modes at ASDEX Upgrade

J.E. Boom[1*], I.G.J. Classen[1], E. Wolfrum[2], P.C. de Vries[1], M. Maraschek[2], A.J.H. Donné[1,3],
B.J. Tobias[4], C.W. Domier[5], N.C. Luhmann Jr.[5], H.K. Park[6],
and the ASDEX Upgrade Team

[1] *FOM Institute for Plasma Physics Rijnhuizen, 3430 BE Nieuwegein, the Netherlands*
[2] *Max-Planck-Institut für Plasmaphysik, 85748 Garching bei München, Germany*
[3] *Technische Universiteit Eindhoven, 5600 MB Eindhoven, The Netherlands*
[4] *Princeton Plasma Physics Laboratory, Princeton, NJ 08540, USA*
[4] *University of California at Davis, Davis, CA 95616, USA*
[5] *POSTECH, Pohang, Gyeongbuk, 790-784, Korea*
* E-mail: J.E.Boom@rijnhuizen.nl

Introduction

In the high confinement mode (H-mode), tokamak operation is usually afflicted by edge localized modes (ELMs) which are triggered by the associated steep pressure gradient and high current density at the edge transport barrier. They expel plasma particles and energy into the scrape-off-layer (SOL) giving rise to high power loads on the divertor target plates and possibly, in case of steady state reactor operation, intolerable erosion. As a beneficial side effect, though, ELMs will also help control the plasma density and impurity accumulation.

The most common ELM regime, so-called type-I, exhibits the aforementioned large peak heat loads. However, ELM regimes with significantly lower energy losses per ELM event have also been observed [1, 2]. One of the small ELM regimes at ASDEX Upgrade (AUG), which combines both good confinement and small energy losses, is the type-II ELM regime [3] (and references therein).

Apart from possibly being an interesting operational scenario for future fusion reactors, understanding the physics that govern the dynamics of these type-II ELMs could also increase the understanding of pedestal stability for type-I ELMs. The exact nature of pedestal stability in the type-II ELM regime is still unknown; it has been proposed, though, that high frequency, low amplitude ELMs appear when the stability lies in between the first and second stable ballooning regimes [4].

In this contribution, the presence of a distinguishing broadband fluctuation near the plasma edge, which typically occurs during the type-II ELMy phase, is further investigated in detail.

ECE-Imaging observations on type-II ELMs at ASDEX Upgrade

The type-II ELM regime at AUG is reached using highly shaped plasmas in double null (DN) configuration. In the actual discharge used for the work presented here, the plasma current was $I_p = 0.8$ MA and the magnetic field $B_t = -2.5$ T. The plasma is predominantly heated by neutral beam injection (NBI) with an input power of up to 7.5 MW; type-I ELMs already occurred at an input power of 5 MW. In order to reach the required DN configuration, ΔR_{sep} (the mid-plane distance between the primary and secondary separatrix) is reduced to 8 mm by slowly shifting the position of the magnetic axis upwards. After that, the plasma has reached its final shape with an upper and lower triangularity of $\delta_{R,up} = 0.46$, $\delta_{R,low} = 0.33$, an elongation of $\kappa = 1.66$, and a q_{95} of -5.4.

As can be seen in **Figure 1** (a), the spiky signature on the divertor thermo-currents (due to the type-I ELMs) disappears, which indicates a reduction of the power loads. Simultaneously, the reduction in confinement is only about 10% and the $H_{98y,2}$ factor does not fall below unity. Under these circumstances, a broadband magnetohydrodynamic activity appears which is characteristic for type-II ELMs, as described by [5, 6], and most recently by [7].
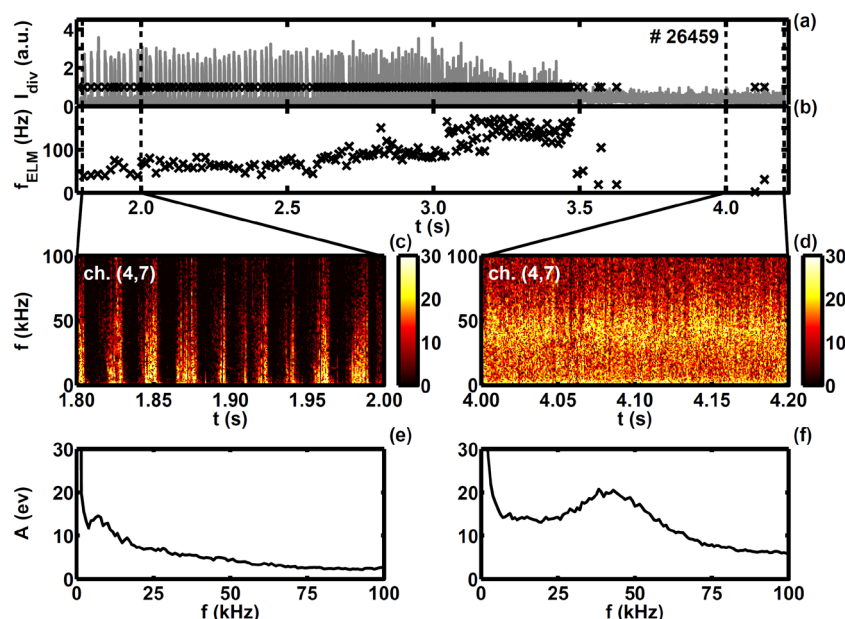
Figure 1. Transition of type-I to -II ELMs: in (a) the peaks in the divertor thermo-current are shown, and in (b) the ELM frequency as determined from these. In (c) and (d) the spectrograms of the type-I and -II phases are shown, and in (e) and (f) the corresponding frequency spectra, averaged over the indicated time-windows.

The main diagnostic that has been used here to study this feature at the plasma edge is ECE-Imaging (ECEI) [8]. ECEI at AUG consists of an array of 16 detectors, each of which serves as a conventional ECE radiometer. The quasi-optical setup allows for the 16 lines of sight to be focussed at the LFS edge with a waist of 1.5 cm at the focal plane. In the radial direction, 8 local oscillator frequencies per line of sight determine the coverage (about 13 cm in the plasma). Therefore, the total area covered is about 40x13 cm^2 (as can be seen in **Figure 2**). The sampling rate of ECEI is set to 200 kHz, which covers the entire length of the discharge. In order to obtain electron temperatures, the measurements are cross-calibrated with the 1D ECE (which is absolutely calibrated).

In **Figure 1** (a, b), the transition of type-I to type-II is shown for the AUG discharge # 26459. With the magnetic axis moving upwards, the type-I ELM frequency slowly increases from 50 to 150 Hz and from 3.7 s onwards the type-I ELMs have completely disappeared. In (c) and (d), two spectrograms of one of the ECEI channels are shown from which the differences between the type-I and -II phase can be seen. In the type-II phase (d), a broadband temperature fluctuation can be seen which is constantly present, whereas this is not the case in the type-I phase (c). There, the plasma edge has to be built up again after each ELM-crash. The difference becomes even more pronounced in (e) and (f), showing the average frequency spectra over the time-windows indicated in (a, b). Here, the broadband fluctuation in (f) clearly stands out.
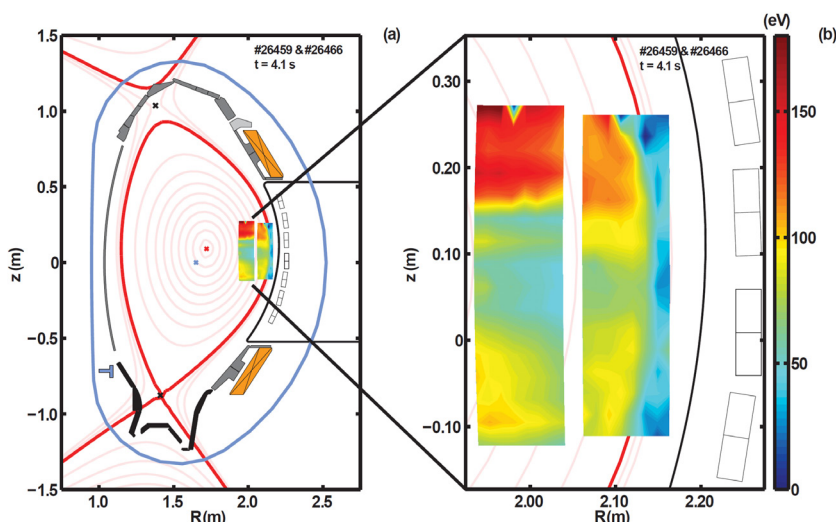

Figure 2. Distribution of the amplitude of the broadband fluctuation: in (a), an overview is shown of the whole cross-section of AUG and the location of the two ECEI measurements. The zoom in (b) shows the spatial distribution of the fluctuations amplitude in more detail.

2

Based on the first ECEI measurements of these fluctuations [7], the experiments have been repeated in two consecutive discharges with the ECEI viewing window set to two neighbouring positions, **Figure 2** (a). In both discharges, a time-window of 22 ms was selected where no type-I ELMs were present (the DN phase in # 26466 was not completely free of type-I ELMs). For all 128 channels, in both discharges, frequency spectra were made similar to the one shown in **Figure 1** (f). Then, for each spectrum, the amplitude in the 30-60 kHz range has been determined; the amplitude distribution, obtained this way, is shown in **Figure 2** (b). Here, it can clearly be seen that, when averaged over time, the distribution is such that there is a minimum between $z = 3$ cm and $z = 14$ cm. Note that, from the equilibrium reconstruction, it was found that the magnetic axis is located at $z = 8$ cm. While this distribution was shown only for the outer ECEI position in [7], it can be seen here to continue towards the plasma centre on the inner ECEI measurement.

In **Figure 3**, the propagation of the T_e fluctuations through the ECEI observation window is shown. Here, in (a) and (c), the temperature has been averaged over all 8 radial channels for each of ECEI's 16 lines of sight (LOS). This way, as is most clearly seen in (c), the propagation of single T_e dips and peaks can be followed as they move from bottom to top (i.e. in the electron diamagnetic drift direction). As can be determined in (c) from the indicative lines (light blue) around $t = 4.1093$ s, the speed of a single T_e peak is about 5.4 km/s; not accounting for plasma rotation.

In (b) and (d), the $\langle T_e \rangle_R$ is normalised and shown for all LOSs put underneath each other. From this perspective, as is most noticeably seen in (b) between 4.106 s and 4.110 s (indicated by the red lines), it seems that there are subsequent periods of high and low amplitude. This is reminiscent of a beat wave resulting from the interference of two waves with marginally different frequencies. If this were the case here, and using the indicative (red) lines in (b), the difference between the two frequencies (i.e. the beat wave's frequency) would be about 1.4 kHz; which is not resolvable from the spectra e.g. shown in **Figure 1**. At 0.5 km/s, the speed with which this overall fluctuation passes by in front of ECEI is a factor of 10 slower than a single T_e peak as shown in (c) and (d).
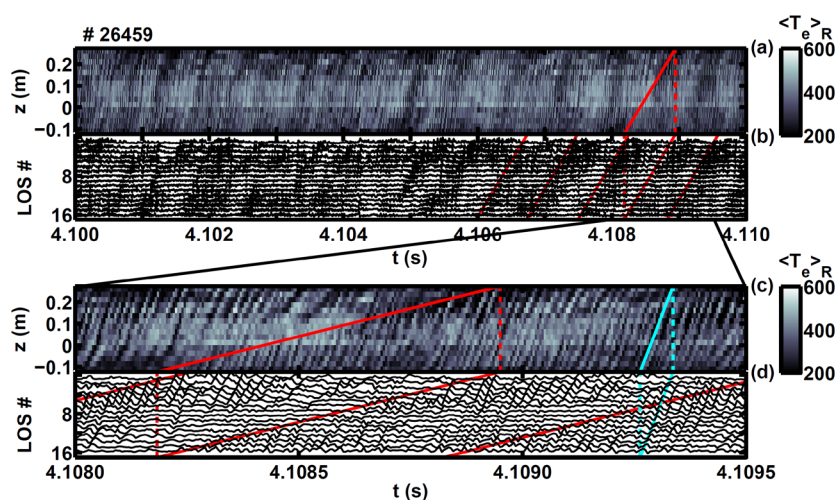

Figure 3. Propagation of T_e fluctuations through the ECEI observation window during the type-II phase of # 26459. In (a) and (c), the mean T_e (averaged over the 8 radial channels per LOS) is shown as a function of time and vertical position. This $\langle T_e \rangle_R$ is normalised and shown for all LOSs put underneath each other in (b) and (d).

Comparison to Mirnov coil measurements

For the measurement of magnetic fluctuations, the Mirnov coils are the diagnostic of choice. Here, the so-called 'ballooning' coil array has been used which is located close to the plasma on the LFS (some of which can be seen in **Figure 2**). These coils measure the perturbations of the radial magnetic field at a constant sampling rate of 2 MHz.

As can be seen from the spectra of these coils, shown in **Figure 4** (a) for the same discharge and time, the broadband fluctuation which is observed by ECEI, is also visible in these measurements. In (b) and (c), the distribution of the broadband fluctuation's amplitude is shown along the array of coils. Comparing these measurements to the observations from ECEI (**Figure 2**), it occurs that a similar amplitude minimum is found only after a background subtraction in the

Figure 4. The spectra of all 14 Mirnov 'ballooning' coils are shown in (a). In (b) and (c) the amplitude of the broadband peak is shown as a function of the vertical position of each coil. The distance of each coil to the magnetic axis is shown in (d).

power spectrum (I_{peak} in **Figure 4** (c)) and not in the total intensity, I_{tot}, of the 30-60 kHz range of the spectrum. Furthermore, the minimum in amplitude is observed between $z = -2.5$ cm and $z = 7.5$ cm. The size of this minimum is similar to that observed by ECEI, but shifted down about 6 cm. In (d) it is shown that the Mirnov coils between $z = -10$ cm and $z = 20$ cm have approximately the same distance from the magnetic axis.
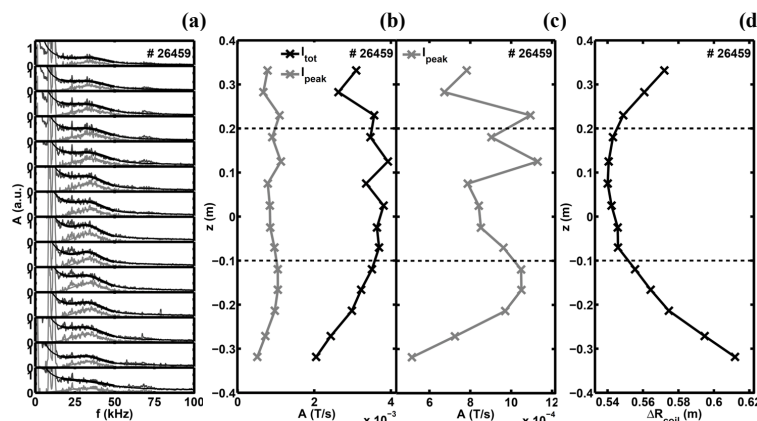
Discussion and outlook

The ECEI measurements presented in this work show (when averaged over time) that the amplitude of a fluctuation typically found in accompaniment with type-II ELMs is not evenly distributed over the poloidal plane. After background subtraction, measurements from the Mirnov coils seem to confirm this observation. The difference in location of the amplitude's minimum could be due to the different toroidal locations of the two diagnostics.

Following T_e fluctuations in time, and along the vertical direction, alternating periods of high and low T_e amplitude were found. This beat wave characteristic might give a clue to the origin of the broadband nature of this fluctuation.

As a next step, measurements from the AXUV diagnostic will also be evaluated in order to find whether the position of the amplitude's minimum is rotating in axisymmetric geometry [7]. Furthermore, a mode with similar features as the one described here for type-II ELMs has been found in discharges with type-I ELMs [9]. A more detailed comparison should reveal whether the two could be of the same origin and to what extent they are related.

References
[1]   Greenwald M *et al.* 1999 *Phys. Plasmas* **6** 1943

[2]   Kamada Y *et al.* 2000 *Plasma Phys. Control. Fusion* **42** A247

[3]   Stober J *et al.* 2005 *Nucl. Fusion* **45** 1213

[4]   Ozeki T *et al.* 1990 *Nucl. Fusion* **30** 1425

[5]   Perez C P *et al.* 2004 *Plasma Phys. Control. Fusion* **46** 61

[6]   von Thun C P P *et al.* 2008 *Plasma Phys. Control. Fusion* **50** 065018

[7]   Wolfrum E *et al.* 2011 *Plasma Phys. Control. Fusion* (accepted)

[8]   Classen I G J *et al.* 2010 *Rev. Sci. Instrum.* **81** 10D929

[9]   Boom J E *et al.* 2011 *Nucl. Fusion* (submitted)